RVB phase of hydrogen at high pressure towards the first *ab-initio* Molecular Dynamics by Quantum Monte Carlo

Claudio Attaccalite

The electronic structure problem

$$\hat{H} = \sum_{i=1}^{N} -\frac{1}{2}\nabla_i^2 + \frac{1}{2}\sum_{\vec{r}_i \neq \vec{r}_j} \frac{1}{|\vec{r}_i - \vec{r}_j|} - \sum_{i}^{N}\sum_{j}^{N_{ions}} \frac{1}{|\vec{r}_i - \vec{R}_j|} + \frac{1}{2}\sum_{\vec{R}_i \neq \vec{R}_j} \frac{1}{|\vec{R}_i - \vec{R}_j|}$$

P.A.M. Dirac: *The fundamental laws necessary for the mathematical treatment of a large part of physics and the whole of chemistry are thus completely known, and the difficulty lies only in the fact that application of these laws leads to equations that are too complex to be solved.*

Why QMC?

Simple empirical potentials

- Force fields, pair potentials…

Intermediate methods

- Tight-binding,
- many-body potentials: EAM

***ab-initio* techniques**

- Hartree-Fock
- Density functional theory (DFT)

Beyond DFT:

- Quantum Monte Carlo
- Quantum Chemical: CI

Outline

- Quantum Monte Carlo
- The trial wave-function
- Optimization Methods
- Results on Molecules
- Molecular Dynamics using QMC forces
- Results on high pressure hydrogen
- New phase in high pressure hydrogen?

Variational Monte Carlo

$$\langle A \rangle_{var} = \frac{\int \Psi_T^*(R) \hat{A} \Psi_T(R) dR}{\int \Psi_T^*(R), \Psi_T(R) dR}$$

Monte Carlo integration is necessary because the wave-function contains explicit particle correlations that leads to non-factoring multi-dimension integrals.

$$\langle A \rangle_{var} = \int P(R) A_L(R) dR$$

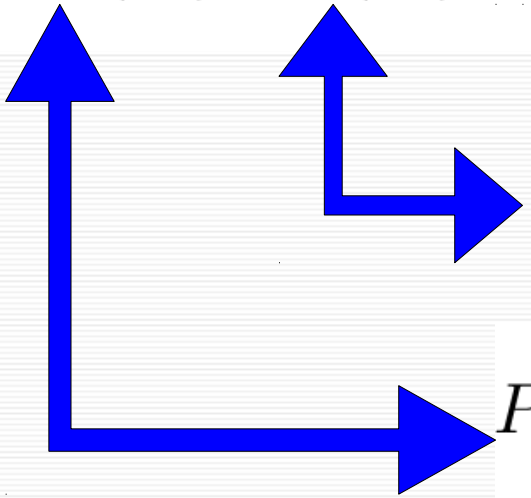

$$A_L(R) = \frac{\hat{A}\Psi_T}{\Psi_T(R)dR}$$

$$P(R) = \frac{|\Psi_T(R)|^2}{\int \Psi_T^*(R)\Psi_T(R)dR}$$

The trial wave-function

The trial-function completely determines quality of the approximation for the physical observables

The JAGP wave-function

$$\Psi(r_1, r_2, \ldots, r_n) = \Phi_{AGP} J_1 J_2 J_3$$

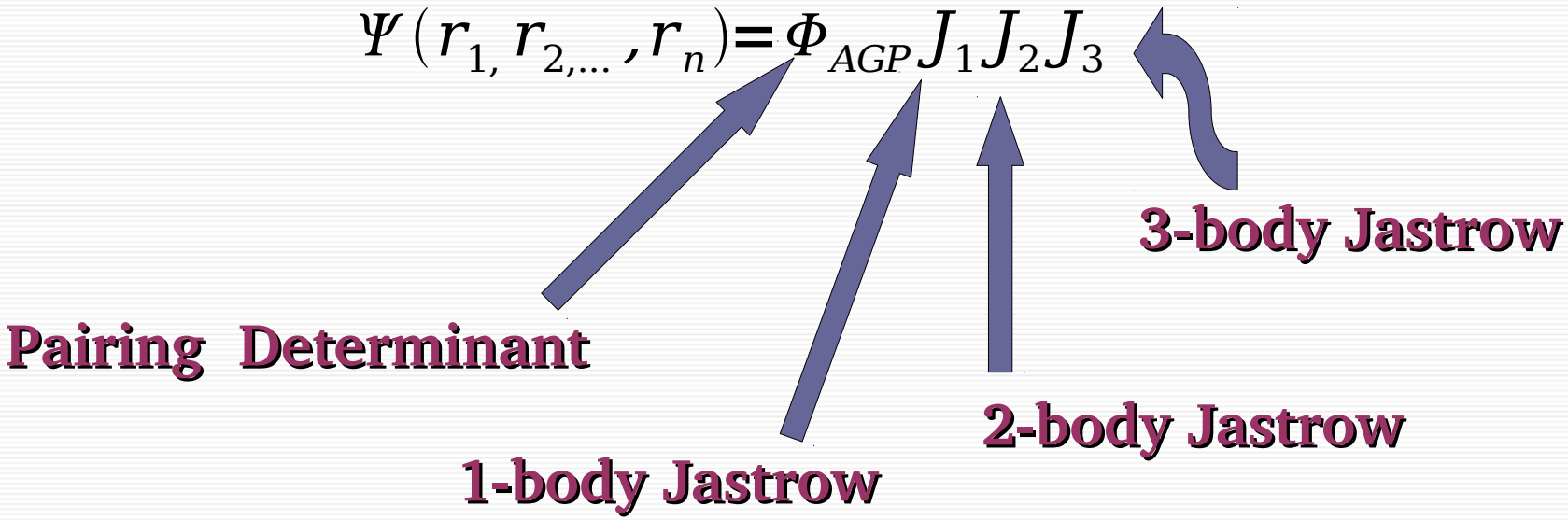

The AGP wave-function

$$\Psi_{AGP}(\vec{r}_1,\ldots,\vec{r}_N) = \det\left(\Phi_{AGP}(\vec{r}_i,\vec{r}_{j+N/2})\right).$$

$$\Phi_{AGP}(\vec{r}^{\uparrow},\vec{r}^{\downarrow}) = \sum_{l,m,a,b} \lambda_{a,b}^{l,m}\phi_{a,l}(\vec{r}^{\uparrow})\phi_{b,m}(\vec{r}^{\downarrow})$$

where
i,j are spin up and down electrons
a,b are different atoms
l,m different orbitals

The matrix $\lambda_{a,b}^{l,m}$ has to be symmetric in order to have a spin singlet

The major advantage of the AGP is that it implicitly contains many
Slater determinants but can be evaluate with the cost of single
determinant N/2 x N/2. (where N=number of electrons).

H_2 molecule and AGP

$$\begin{aligned}\Psi_{H_2} &= \lambda_{11}\phi^A_{1s}(r_1)\phi^A_{1s}(r_2) + \lambda_{22}\phi^B_{1s}(r_1)\phi^B_{1s}(r_2) \\ &+ \lambda_{12}\phi^A_{1s}(r_1)\phi^B_{1s}(r_2) + \lambda_{21}\phi^B_{1s}(r_1)\phi^A_{1s}(r_2)\end{aligned}$$

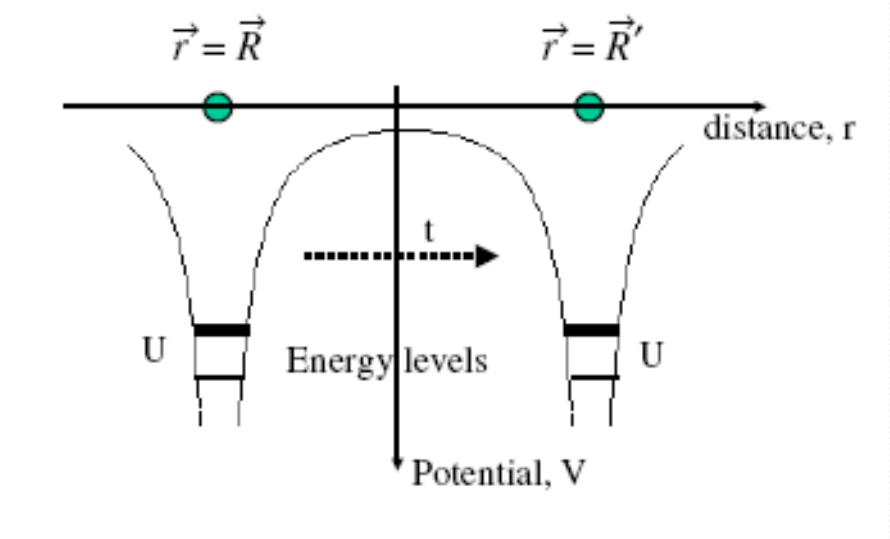

The one-body Jastrow factor

$$-\psi'' - \frac{1}{r}\left(Ze^2\psi + \psi'\right) = E\psi \quad \Longrightarrow \quad \frac{1}{\psi}\psi' = -Ze^2$$

It's difficult satisfy nuclear cusp conditions
with the pairing determinant

$$J_1(\vec{r}_1, ..., \vec{r}_N) = \exp\left[\sum_{i,a}^{N} \left(\xi_a(\vec{r}_i) + \Xi_a(\vec{r}_{ia})\right)\right],$$

where: $\psi_{a,i}(\vec{r}) - \psi_{a,i}(\vec{R}_a) \simeq |\vec{r} - \vec{R}_a|^2$

Nuclear cusp: $\xi_a(r) = \dfrac{-Z_a r}{(1 + br)}$

The two-body Jastrow

As for the nuclear-cusp

$$J_2(\vec{r}_1, ..., \vec{r}_N) = \exp\left(\sum_{i<j}^{N} u(r_{ij})\right)$$

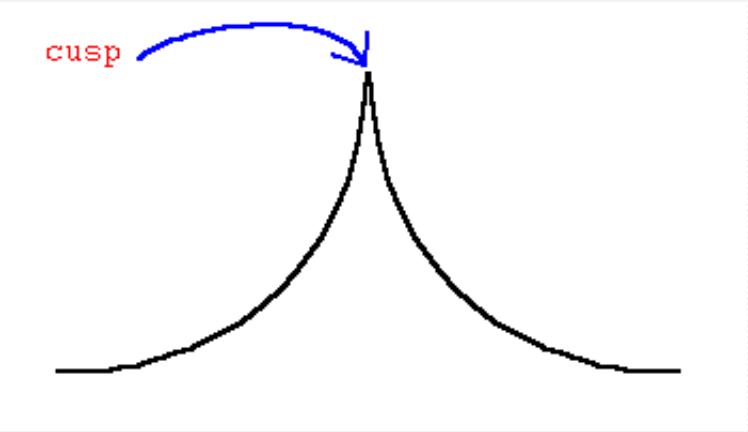

where $u(r) = \dfrac{r}{2(1+br)}$

In this functional form the cusp condition for anti-parallel spin electrons is satisfied, whereas the one for parallel spins is neglected in order to avoid the spin contamination

The Three-body Jastrow

$$J_3(\vec{r}_1, ..., \vec{r}_N) = \exp\left(\sum_{i<j} \Phi_J(\vec{r}_i, \vec{r}_j)\right)$$

$$\Phi_J(\vec{r}_i, \vec{r}_j) = \sum_{l,m,a,b} g_{l,m}^{a,b} \psi_{a,l}(\vec{r}_i) \psi_{b,m}(\vec{r}_j)$$

The three-body Jastrow factor:

- describes Van Der Waals forces
- suppress superconductivity
- describes Mott insulators
- keeps charge constant on atoms or molecules (not fixed by AGP)

The three-body Jastrow factor must:

- preserve nuclear and electronic cusp conditions
- whenever the atomic distances are large it factorizes into a product of independent contributions located near each atom

Geminal expansion and orbitals

$$\Phi_J(\vec{r}_i,\vec{r}_j) = \sum_{l,m,a,b} g_{l,m}^{a,b}\psi_{a,l}(\vec{r}_i)\psi_{b,m}(\vec{r}_j)$$

$$\Phi_{AGP}(\vec{r}^{\uparrow},\vec{r}^{\downarrow}) = \sum_{l,m,a,b} \lambda_{a,b}^{l,m}\phi_{a,l}(\vec{r}^{\uparrow})\phi_{b,m}(\vec{r}^{\downarrow})$$

$$\Phi(\vec{r}) = C_1 \mathrm{e}^{-Z_1|\vec{r}|} Y_{l,m}$$

$$\Phi(\vec{r}) = C_1 \mathrm{e}^{-Z_1|\vec{r}|^2} Y_{l,m}$$

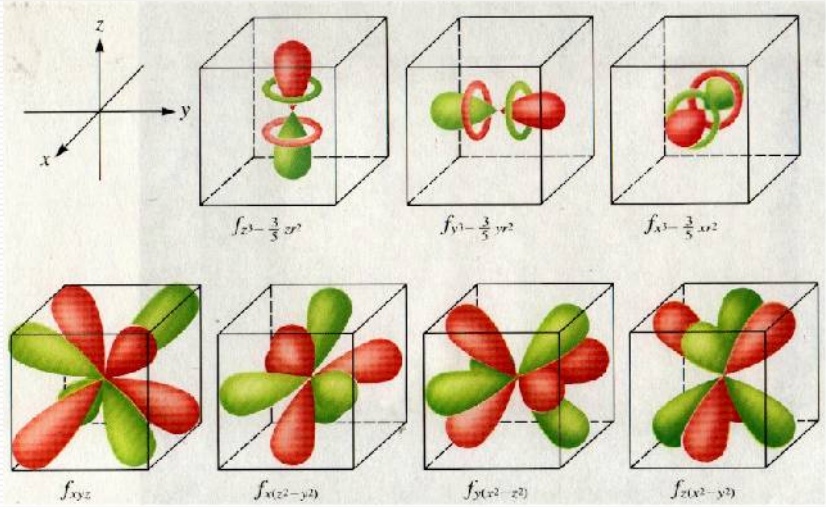

Stochastic Reconfiguration 1

$$|\Psi_P\rangle = \left(\Lambda - \hat{H}(\alpha'_k ... \alpha_p)\right)|\Psi_T\rangle$$

$$|\Psi'_T\rangle = \delta\alpha_0|\Psi_T\rangle + \sum_{k=1}^{p} \delta\alpha_k \frac{\partial}{\partial\alpha_k}|\Psi_T\rangle$$

In the Stochastic Reconfiguration one adjusts the parameters
of the original trial-function to be closer as much as possible to the projected one.

$$\hat{O}_k \Psi_T(x) = \frac{\partial}{\partial\alpha_k} \ln \Psi_T(x) \text{ and } \hat{O}_0 = \hat{I}$$

$$\Psi'_T = \sum_{k=0}^{p} \delta\alpha_k \hat{O}_k \Psi_T$$

Stochastic Reconfiguration 2

we require that a set of mixed average correlation functions, corresponding to the two wave-functions are equal:

$$\frac{\langle \Psi_T | \hat{O}_k | \Psi'_T \rangle}{\langle \Psi_T | \Psi'_T \rangle} = \frac{\langle \Psi_T | \hat{O}_k | \Psi_P \rangle}{\langle \Psi_T | \Psi_P \rangle}$$

this is equivalent to

$$\delta\alpha_0 + \sum_{l=1} \delta\alpha_l \langle \hat{O}^l \rangle = \Lambda - \langle \hat{H} \rangle$$

$$\delta\alpha_0 \langle \hat{O}^k \rangle + \sum_{l=1} \delta\alpha_l \langle \hat{O}^k \hat{O}^l \rangle = \Lambda \langle \hat{O}^k \rangle - \langle \hat{O}^k \hat{H} \rangle \text{ for } k \neq 0$$

substituting the first equation in the others we obtain

$$\sum_{l=1} \delta\alpha_l \langle (\hat{O}^k - \langle \hat{O}^k \rangle)(\hat{O}^l - \langle \hat{O}^l \rangle) \rangle = \langle \hat{O}^k \rangle \langle \hat{H} \rangle - \langle \hat{O}^k \hat{H} \rangle$$

Stochastic Reconfiguration 3

in analogy with the steepest descent

$$\sum_{l=1} \delta\alpha_l s_{kl} = f_k$$

where

$$s_{kl} = \langle (\hat{O}^k - \langle \hat{O}^k \rangle)(\hat{O}^l - \langle \hat{O}^l \rangle) \rangle \qquad f_k = -\frac{\partial E}{\partial \alpha_k} = -\frac{\langle \Psi | O_k H + H O_k | \Psi \rangle}{\langle \Psi | \Psi \rangle}$$

at each interaction the wave function parameters are iteratively updated according to

$$\alpha_i^{new} = \alpha_i^{old} + \sum_i \bar{s}_{i,k}^{-1} f_k \Delta t$$

the energy variation for a small change of the parameters is

$$\Delta E = -\Delta t \sum_{i,j} \bar{s}_{i,j}^{-1} f_i f_j + O(\Delta t^2)$$

Noise and Optimization

Stochastic Reconfiguration is similar to a Langevin dynamics in the parameters space.

where $\frac{T^{eff}}{2} = \langle \eta^2 \rangle$ and $\langle \eta^2 \rangle \sim 1/(number\ of\ VMC\ steps)$

to reduce statistical fluctuations we averages parameters values after the equilibration
and increase the number of steps in the VMC simulations

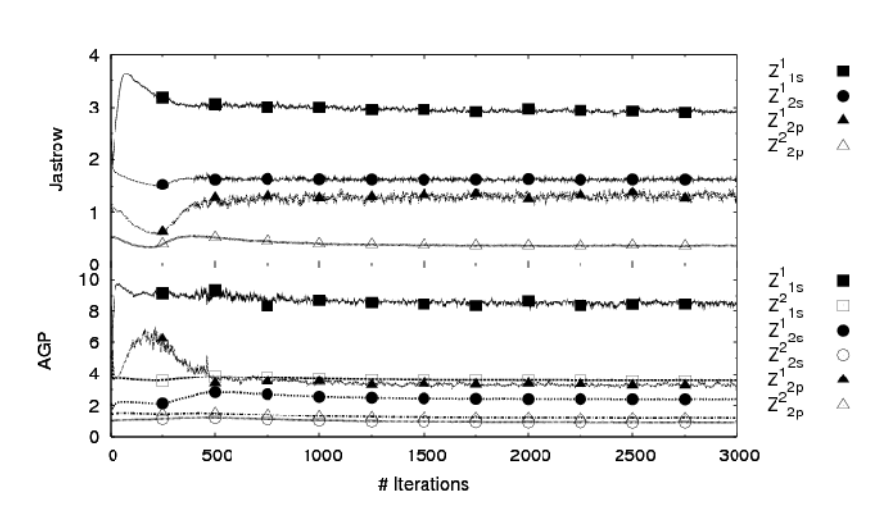

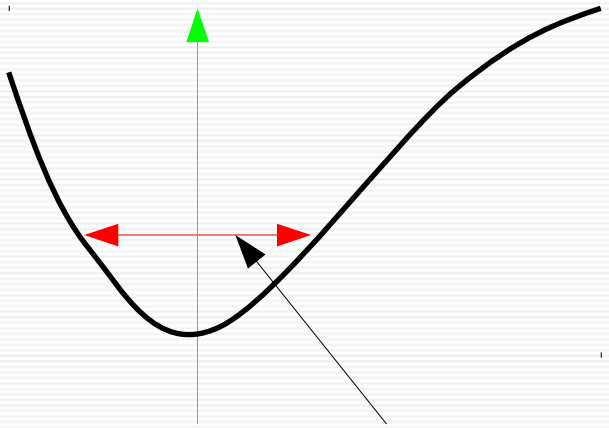

thermal fluctuations

In the limit of infinite bin length the Euler conditions are satisfied exactly

Resonance in Benzene

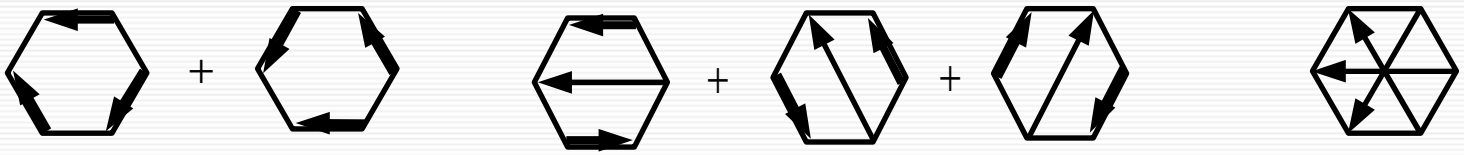

Kekule’ Dewar Claus-Armstrong Baeyer

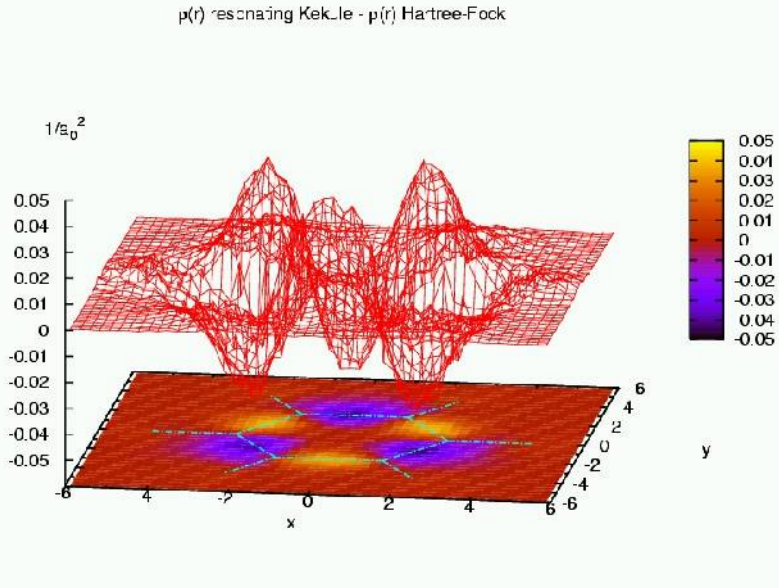

TABLE IV: Binding energies in eV obtained by variational (Δ_{VMC}) and diffusion (Δ_{DMC}) Monte Carlo calculations with different trial wave functions for benzene. In order to calculate the binding energies yielded by the 2-body Jastrow we used the atomic energies reported in Ref. 10. The percentages ($\Delta_{VMC}(\%)$ and $\Delta_{DMC}(\%)$) of the total binding energies are also reported.

	Δ_{VMC}	$\Delta_{VMC}(\%)$	Δ_{DMC}	$\Delta_{DMC}(\%)$
Kekule + 2body	−30.57(5)	51.60(8)	–	–
resonating Kekule + 2body	−32.78(5)	55.33(8)	–	–
resonating Dewar Kekule + 2body	−34.75(5)	58.66(8)	−56.84(11)	95.95(18)
Kekule + 3body	−49.20(4)	83.05(7)	−55.54(10)	93.75(17)
resonating Kekule + 3body	−51.33(4)	86.65(7)	−57.25(9)	96.64(15)
resonating Dewar Kekule + 3body	−52.53(4)	88.67(7)	−58.41(8)	98.60(13)
full resonating + 3body	−52.65(4)	88.869(7)	−58.30(8)	98.40(13)

Forces with finite variance

the bare force

$$F_A^\nu = -\frac{\partial}{\partial R_i^x} V(r_1,..,r_N;R_1,...,R_m) = -Z_A \sum_{i\neq A}^{M} \frac{Z_i(R_A^\nu - R_i^\nu)}{R_{Ai}^3} - Z_A \sum \frac{(\vec{r}_j - \vec{R}_A^\nu)}{|r_j - R_A|^3},$$

in order to overcome this problem we follow the idea of Assaraf and Caffarel we added another operator with zero expectation value and finite variance

$$\tilde{F} = F + \left[\frac{\tilde{H}\tilde{\Psi}}{\tilde{\Psi}} - \frac{\tilde{H}\Psi_T}{\Psi_T}\right]\frac{\tilde{\Psi}}{\Psi_T}$$

the simplest choice to cancel the divergence in the force is:

$$\begin{aligned} \tilde{H} &= H \\ \tilde{\Psi} &= Q\Psi_T \end{aligned} \qquad Q_A^\nu = Z_A \sum_{i=1}^{N_{elect}} \frac{(x_i^\nu - R_A^\nu)}{\left|\vec{r}_i - \vec{R}_A\right|}$$

$$\tilde{F}_A^\nu = -Z_A \sum_{i\neq A}^{M} \frac{Z_i(R_i^\nu - R_A^\nu)}{R_{Ai}^3} - \frac{\vec{\nabla} Q_A^\nu \cdot \vec{\nabla}\Psi_T}{\Psi_T}$$

Structure Optimization

using the stochastic reconfiguration

$$\sum_{l=1} \delta\alpha_l s_{kl} = f_k$$

with

$$\begin{aligned}
\vec{F}(\vec{R}_a) &= -\vec{\nabla}_{\vec{R}_a} E(\{c_i\}, \vec{R}_a) \\
&= -\frac{\langle\Psi|O_R H + H O_R + \partial_R H|\Psi\rangle}{\langle\Psi|\Psi\rangle} + 2\frac{\langle\Psi|O_R|\Psi\rangle\langle\Psi|H|\Psi\rangle}{\langle\Psi|\Psi\rangle^2},
\end{aligned}$$

Li_2 bonding length

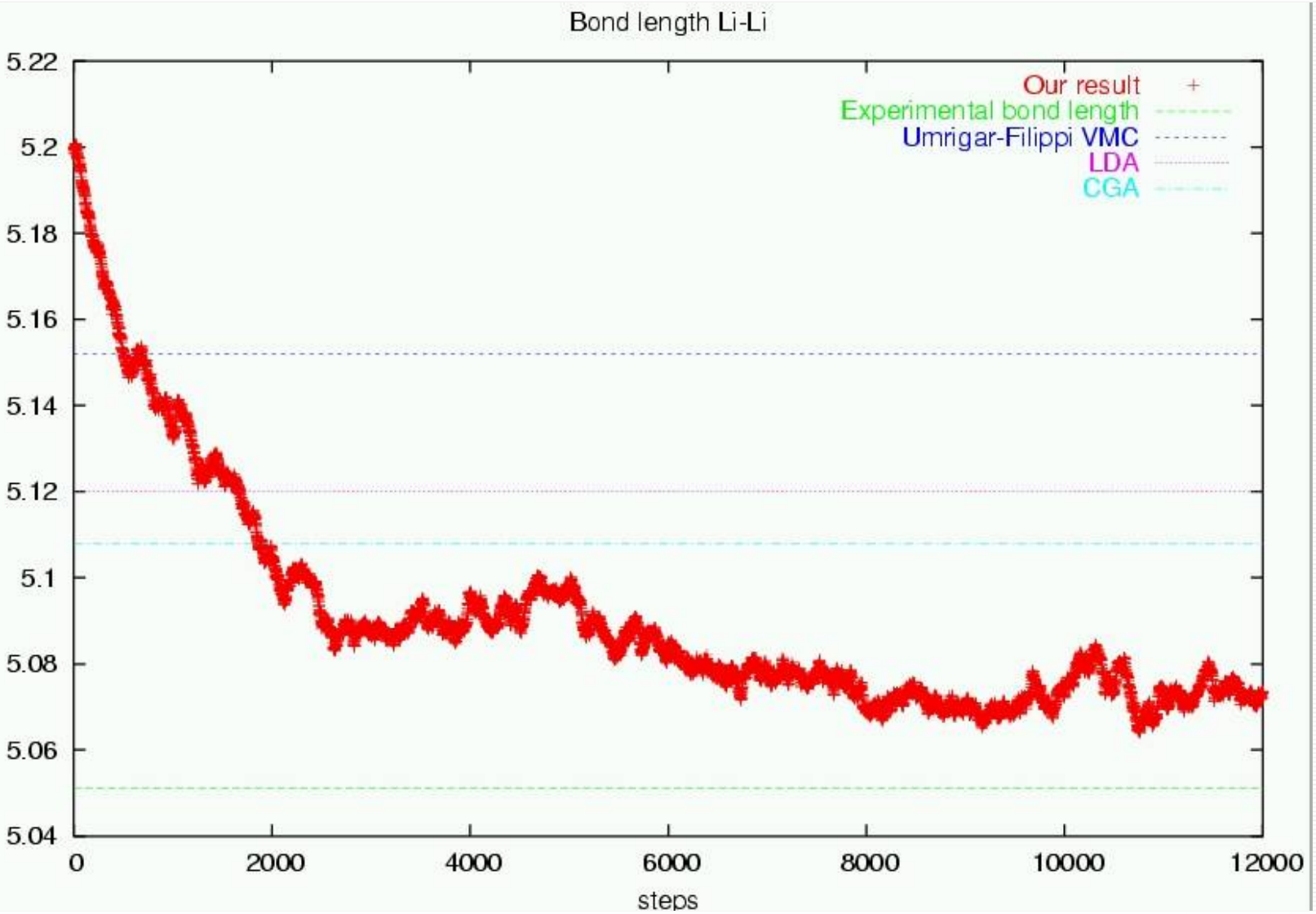

Benzene Structure

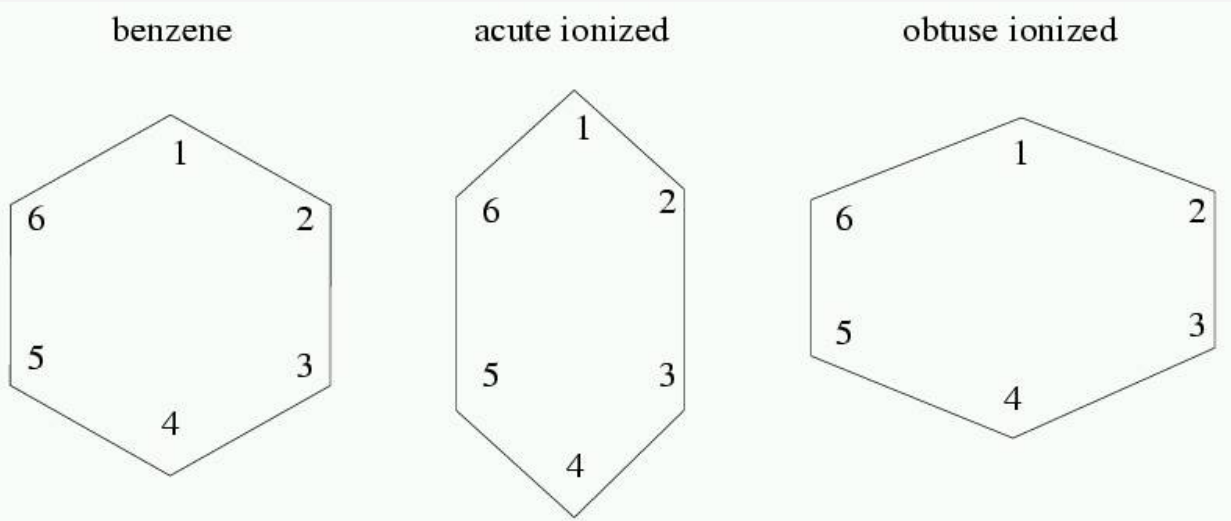

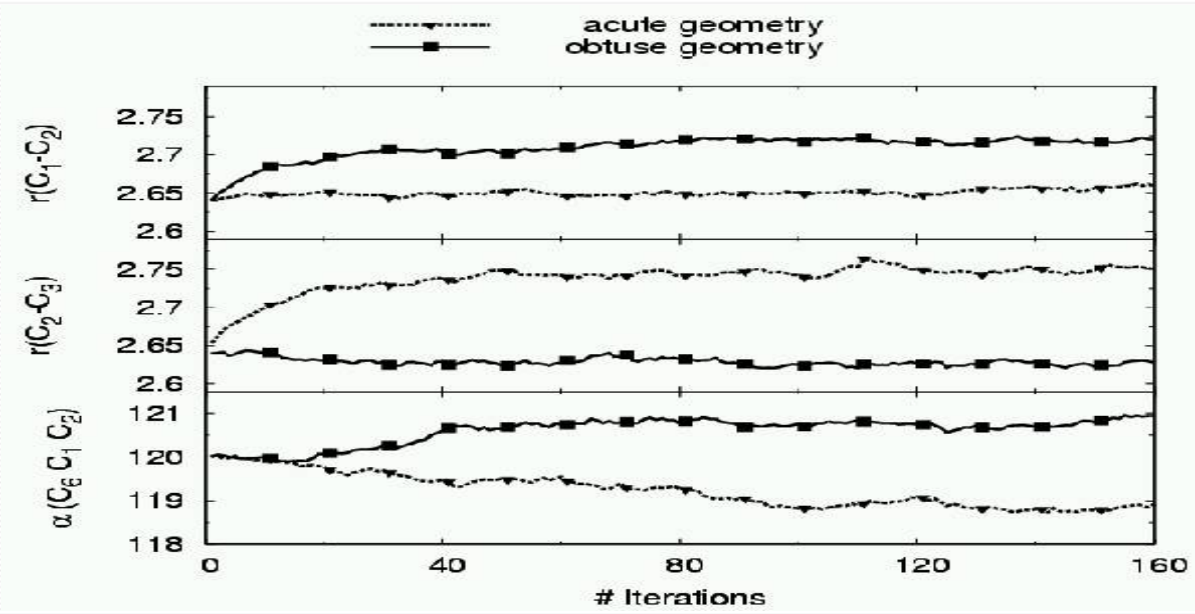

Structure optimization results

TABLE III: Bond lengths (R) in atomic units; the subscript 0 refers to the "exact" results. For the water molecule R is the distance between O and H and θ is the angle HOH (in deg), for CH_4 R is the distance between C and H and θ is the HCH angle.

	R_0	R	θ_0	θ
Li_2	5.051	5.0516(2)		
O_2	2.282	2.3425(18)		
C_2	2.348	2.366(2)		
H_2O	1.809	1.8071(23)	104.52	104.74(17)
CH_4	2.041	2.049(1)	109.47	109.55(6)
	R_0^{CC}	R^{CC}	R_0^{CH}	R^{CH}
C_6H_6	2.640	2.662(4)	2.028	1.992(2)

Results on molecules 1

TABLE I: Total energies in variational (E_{VMC}) and diffusion (E_{DMC}) Monte Carlo calculations; the percentages of correlation energy recovered in VMC ($E_c^{VMC}(\%)$) and DMC ($E_c^{DMC}(\%)$) have been evaluated using the "exact" (E_0) and Hartree–Fock (E_{HF}) energies from the references reported in the table. Here "exact" means the ground state energy of the non relativistic infinite nuclear mass hamiltonian. The energies are in *Hartree*.

	E_0	E_{HF}	E_{VMC}	$E_c^{VMC}(\%)$	E_{DMC}	$E_c^{DMC}(\%)$
Li	-7.47806^a	-7.432727^a	$-7.47721(11)$	98.12(24)	$-7.47791(12)$	99.67(27)
Li_2	-14.9954^c	-14.87152^c	$-14.99002(12)$	95.7(1)	$-14.99472(17)$	99.45(14)
Be	-14.66736^a	-14.573023^a	$-14.66328(19)$	95.67(20)	$-14.66705(12)$	99.67(13)
Be_2	$-29.33854(5)^c$	-29.13242^c	$-29.3179(5)$	89.99(24)	$-29.33341(25)$	97.51(12)
O	-75.0673^a	-74.809398^a	$-75.0237(5)$	83.09(19)	$-75.0522(3)$	94.14(11)
H_2O	$-76.438(3)^b$	$-76.068(1)^b$	$-76.3803(4)$	84.40(10)	$-76.4175(4)$	94.46(10)
O_2	-150.3268^c	-149.6659^c	$-150.1992(5)$	80.69(7)	$-150.272(2)$	91.7(3)
C	-37.8450^a	-37.688619^a	$-37.81303(17)$	79.55(11)	$-37.8350(6)$	93.6(4)
C_2	$-75.923(5)^c$	-75.40620^c	$-75.8273(4)$	81.48(8)	$-75.8826(7)$	92.18(14)
CH_4	-40.515^d	-40.219^d	$-40.4627(3)$	82.33(10)	$-40.5041(8)$	96.3(3)
C_6H_6	$-232.247(4)^e$	$-230.82(2)^f$	$-231.8084(15)$	69.25(10)	$-232.156(3)$	93.60(21)

[a] Exact and HF energies from Ref. 50.
[b] Ref. 51.
[c] Ref. 29.
[d] Ref. 33.
[e] Estimated "exact" energy from Ref. 43.
[f] Ref. 52.

Results on molecules 2

Table 3.3: Binding energies in eV obtained by variational (Δ_{VMC}) and diffusion (Δ_{DMC}) Monte Carlo calculations; Δ_0 is the "exact" result for the non-relativistic infinite nuclear mass Hamiltonian. Also the percentages ($\Delta_{VMC}(\%)$ and $\Delta_{DMC}(\%)$) of the total binding energies are reported.

	Δ_0	Δ_{VMC}	$\Delta_{VMC}(\%)$	Δ_{DMC}	$\Delta_{DMC}(\%)$
Li_2	-1.069	-0.967(3)	90.4(3)	-1.058(5)	99.0(5)
O_2	-5.230	-4.13(4)	78.9(8)	-4.56(5)	87.1(9)
H_2O	-10.087	-9.704(24)	96.2(1.0)	-9.940(19)	98.5(9)
C_2	-6.340	-5.530(13)	87.22(20)	-5.74(3)	90.6(5)
CH_4	-18.232	-17.678(9)	96.96(5)	-18.21(4)	99.86(22)
C_6H_6	-59.25	-52.53(4)	88.67(7)	-58.41(8)	98.60(13)

Simulation of Extended Systems

Hamiltonian with periodic boundary conditions

$$\hat{H} = \sum_{i=1}^{N} -\frac{1}{2}\nabla_i^2 + \frac{1}{2}\sum_{\vec{r}_i \neq \vec{r}_j + \vec{R}_s, \vec{R}_s} \frac{1}{|\vec{r}_i - \vec{r}_j - \vec{R}_s|} - \sum_{\vec{R}_s}\sum_{i}^{N}\sum_{j}^{N_{ions}} \frac{1}{|\vec{r}_i - \vec{R}_j - \vec{R}_s|}$$

$$+ \frac{1}{2}\sum_{\vec{R}_i \neq \vec{R}_j + \vec{R}_s, \vec{R}_s} \frac{1}{|\vec{R}_i - \vec{R}_j - \vec{R}_s|}$$

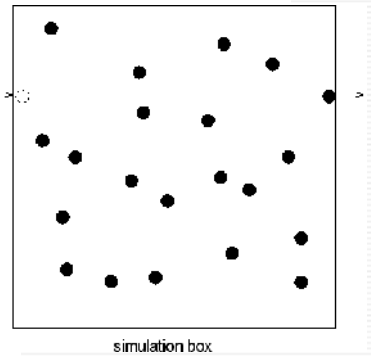

and Ewald 's sums

$$U = \frac{1}{2}\sum_{i,j}^{N}\sum_{R_s} \frac{q_i q_j}{\vec{r}_{ij} + \vec{R}_s} erfc\left(\sqrt{\alpha}(\vec{r}_{ij} + \vec{R}_s)\right)$$

$$+ \frac{1}{2}\sum_{\vec{k}\neq 0}\sum_{i,j}^{N} \frac{4\pi q_i q_j}{V|\vec{k}|^2} e^{i\vec{k}(\vec{r}_i - \vec{r}_j)} e^{-\vec{k}^2/4\alpha} - \sqrt{\frac{\alpha}{\pi}}\sum_{i=1}^{N} q_i^2$$

Periodic Wave-Function

$$\Psi(\vec{r}_1, \vec{r}_2, \ldots) = e^{-i\vec{k}\sum_i \vec{r}_i}\Phi(\vec{r}_1, \vec{r}_2, \ldots)$$

$\vec{k} = 0$

Periodic coordinates
no need of Ewald's sum

$$x_i' = \frac{L}{\pi}\sin\left(\frac{\pi x_i}{L}\right)$$

$$r' = \frac{L}{\pi}\sqrt{\sum_{i=1}^{3}\sin^2\left(\frac{\pi x_i}{L}\right)}$$

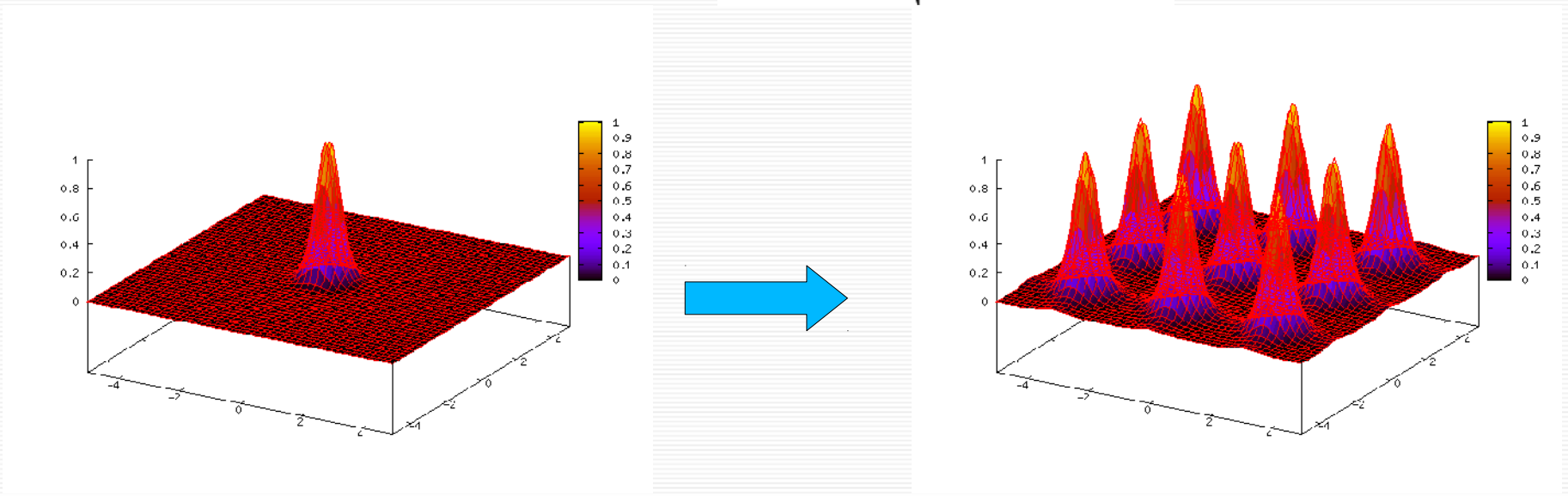

Forces in Periodic Systems

zero-variance principle in periodic systems

$$\begin{aligned} \tilde{\Psi}_{PBC} &= Q_{PBC}\Psi_T \\ Q^{\nu}_{PBC} &= Z_A \sum_{i=1}^{N_{elect}} \frac{\frac{L}{2\pi}\sin\left(\frac{2\pi}{L}(x_\nu - R^{\nu}_A)\right)}{r'_{iA}} \end{aligned}$$

renormalized force

$$\tilde{F}^{\nu} = F^{\nu}_{bare} - \frac{1}{2}\nabla^2 Q^{\nu}_{PBC} - \frac{\vec{\nabla}Q^{\nu}_{PBC}\vec{\nabla}\Psi_T}{\Psi_T}$$

Comparison with other results

Table 6.1: Total energies in variational (E_{VMC}) and diffusion (E_{DMC}) Monte Carlo calculations for 16 hydrogen atoms in a BCC lattice at Rs=1.31 and T=0 (i.e. frozen ion positions). The energies are in *Hartree* for atom.

WF	E_{VMC}	σ^2_{VMC}	E_{DMC}
SJ	-0.4742(2)	0.0764(2)	-0.4857(1)
$SJ3B$	-0.4857(2)	0.0274(2)	-0.4900(1)
LDA	-0.4870(10)		-0.4890(5)
$JAGP$	-0.4871(5)	0.0700(1)	-0.49019(5)
$JAGP-reduced$	-0.4846(2)	0.067(1)	-0.4880(1)

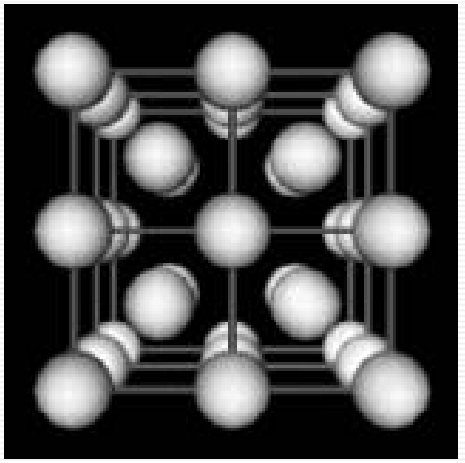

Noise in QMC

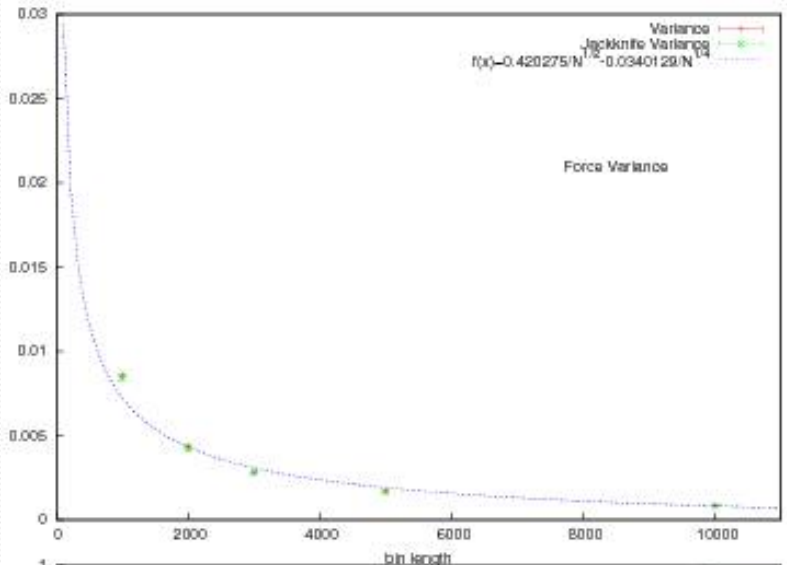
Variance
Jackknife Variance
f(x)=0.420275/N^1/2 -0.0340129/N^1/4
Force Variance
bin length

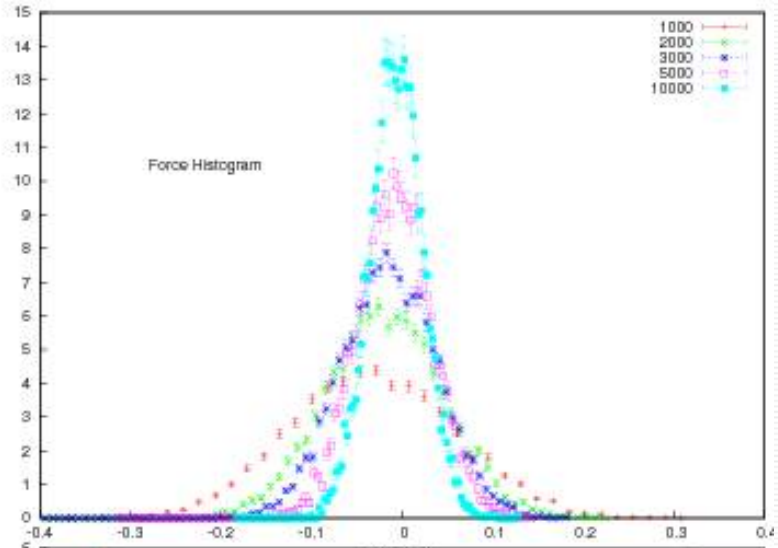
1000
2000
3000
5000
10000
Force Histogram
bin length

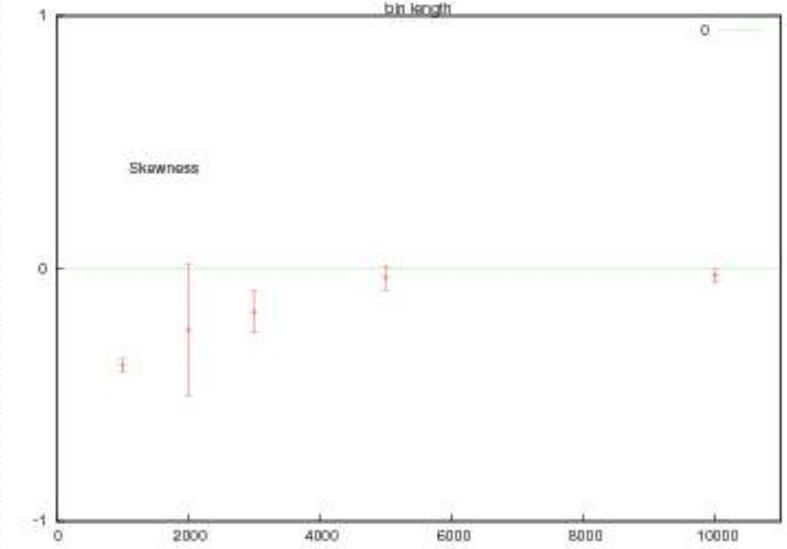
Skewness

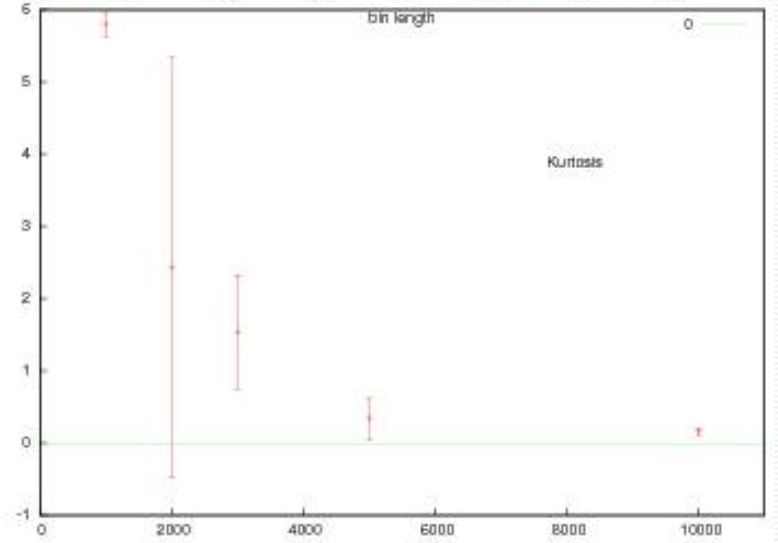
Kurtosis

Finite Temperature Simulation

It is possible to use the forces noise to produce
a finite temperature using
a Generalized Langevin Equation

$$\langle \Gamma_i(t)\Gamma_j(t')\rangle = \alpha_{ij}(x)\delta(t-t')$$
$$\langle \Gamma_i(t)\rangle = 0.$$

$$\begin{cases} \dot{v}_i(t) = -\gamma_{ij}(x)v_j(t) + \frac{f_i(x(t))}{m_i} + \Gamma_i(t) \\ \dot{x}_i(t) = v_i(i) \end{cases}$$

$$\gamma_{ij}(x) = \frac{\alpha_{ij}(x)}{2}\beta m_j$$

$$W_{eq}(x,v) = e^{\frac{-\sum_i \frac{m_i v_i^2}{2} - V(x)}{KT}}$$

Integration of the Langevin Dynamics

$$\dot{v}_i(t) = -\gamma_j v_j(t) + \frac{f_i(x(t))}{m_i} + \Gamma_i(t)$$

The Impulse integrator (R.D. Skeel, J. A. Izaguirre 2002)

$$r^{n+1} = (1 + e^{-\Lambda\Delta})r^n - e^{-\Lambda\Delta}r^{n-1} + \frac{\Delta}{\Lambda}(I - e^{-\Lambda\Delta})g_n$$

$$g = \frac{f}{m} + \Gamma$$

major advantage is stable for large friction

$$A = L\Lambda L^T$$

generalization to non diagonal friction

$$L^T\dot{v} + \Lambda L^T v = L^T g \quad \rightarrow \quad w = L^T v \quad \rightarrow \quad \dot{w} + \Lambda w = L^T g$$

Temperature and Pressure

In the Generalized Langevin Dynamics
the temperature can be estimated at posteriori by equality

$$\frac{3}{2}K_B T = \frac{1}{2}M\langle V^2 \rangle$$

Pressure

$$P_{elect} = \frac{1}{3V}\left[2\frac{\langle E'_{kin}\rangle}{L^2} + \frac{\langle E'_{pot}\rangle}{L}\right] + \frac{2}{3V}\left[\langle O_L H\rangle - \langle O_L\rangle\langle H\rangle\right]$$

$$P_{ionic} = \frac{2N}{3V}\langle E_k^{ionic}\rangle$$

SR optimization with Hessian acceleration

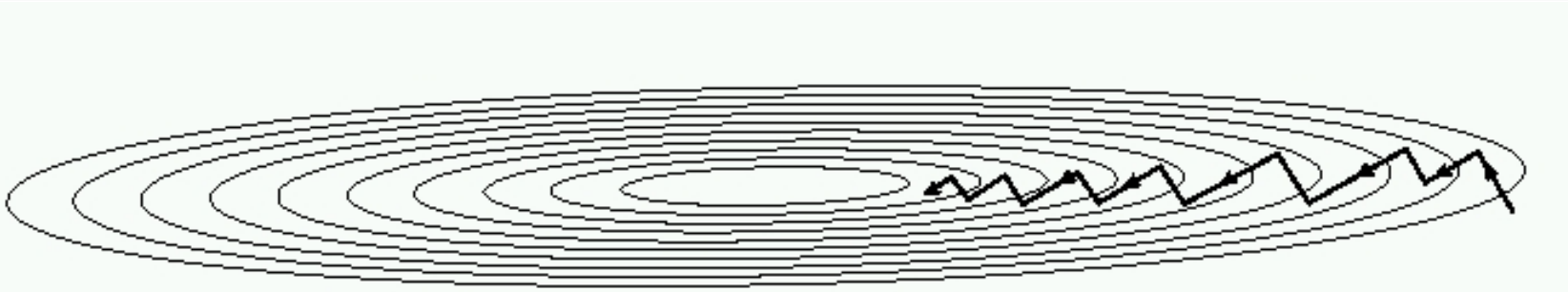

Using Hessian matrix information
to accelerate the convergence

$$\vec{\gamma} = B^{-1}\vec{f} \qquad B = H + \mu S$$

in order to have a stable optimization
the variation of the WF has to be small

$$|\Delta WF|^2 = \langle \phi_\alpha | \phi_{\alpha+\gamma} \rangle = \sum_{k,k'} \gamma_k \gamma_{k'} S^{k,k'}$$

Time-Step Error 1

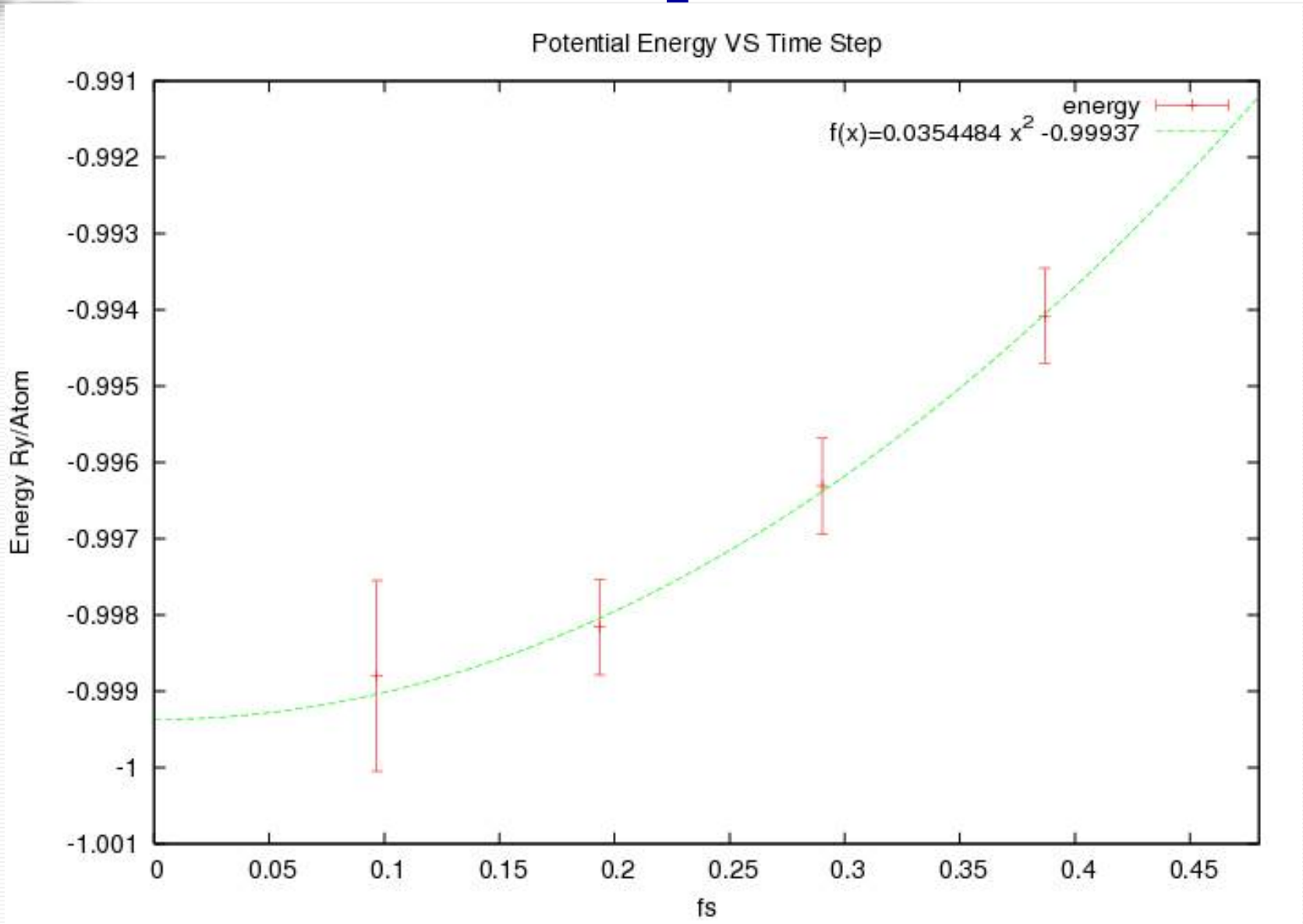

Phase Diagram of Hydrogen

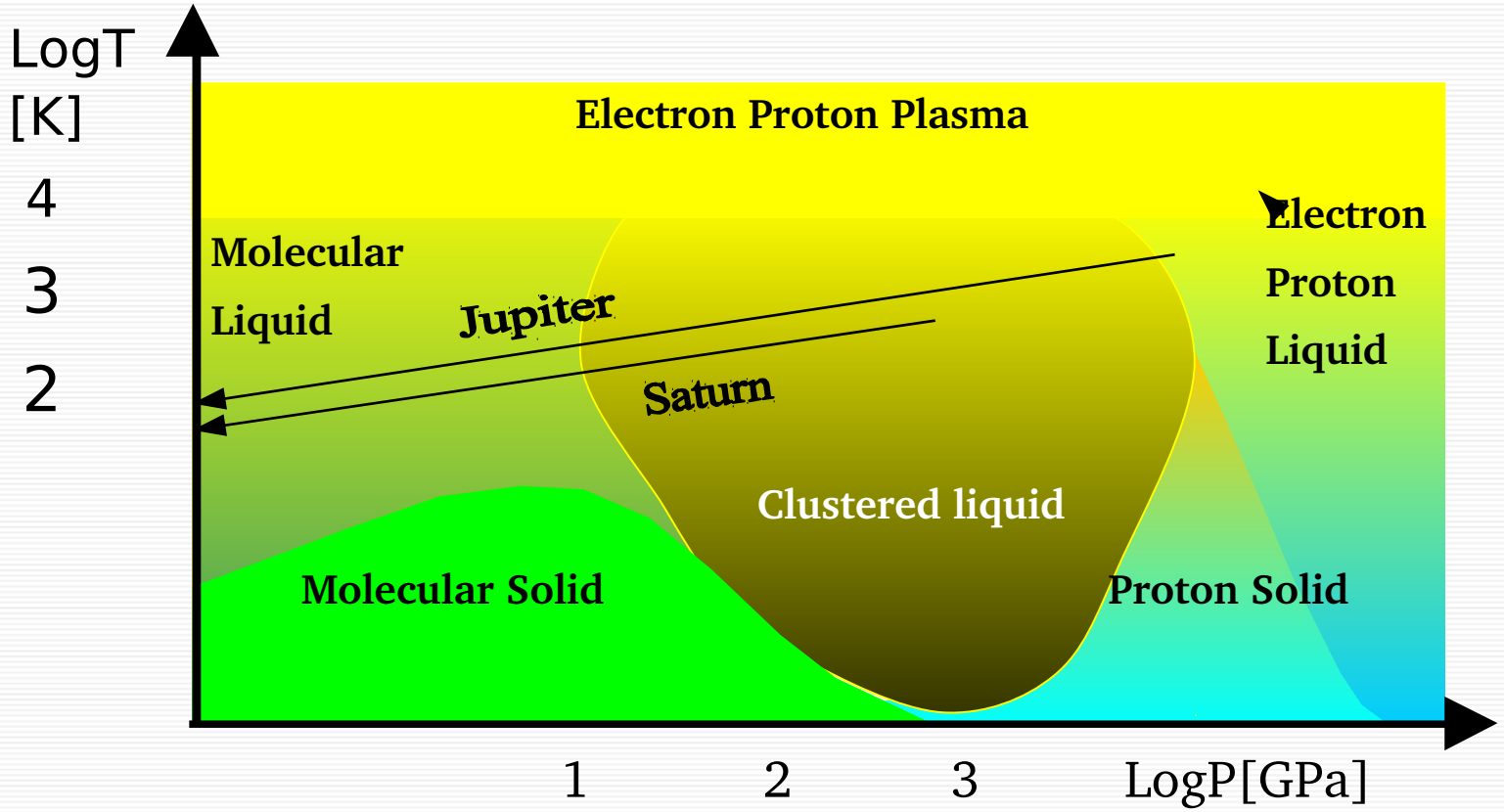

High pressure hydrogen

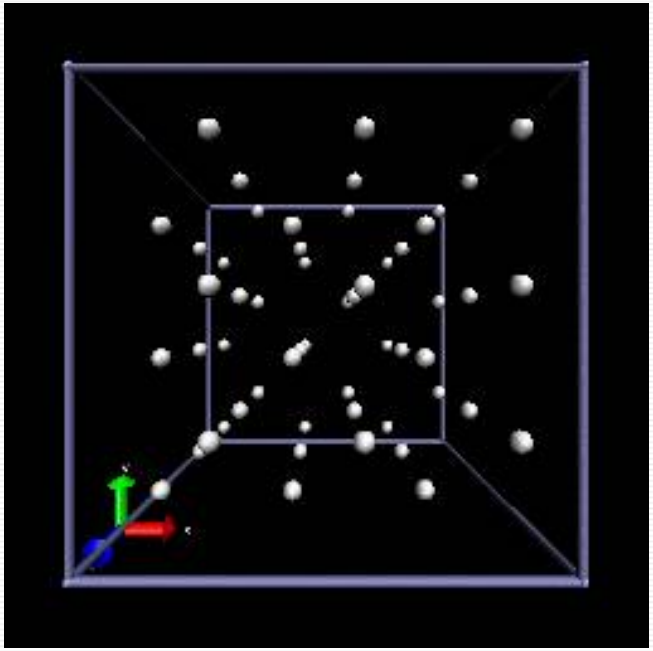

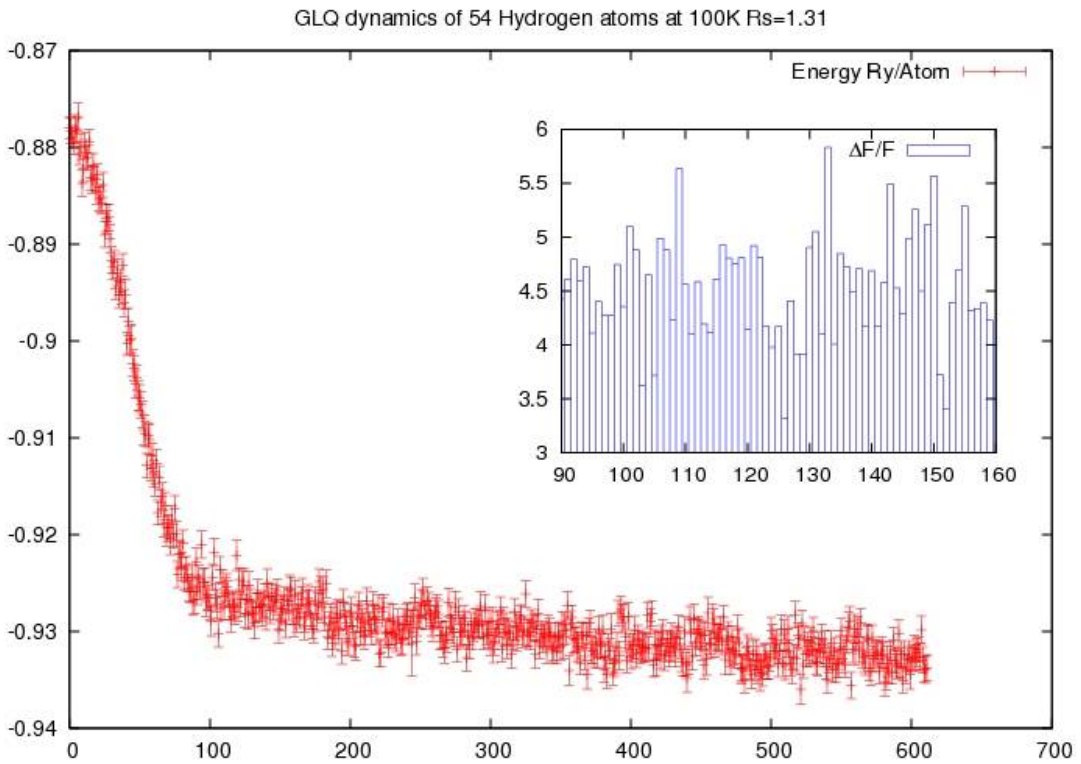

Comparison with other result

Table 6.2: Pressure at different temperatures and densities. We report also the pressure obtained with Gasgun experiment (4), with Silvera-Goldman empirical potential model (5) and CEICM method (6) at Γ point. The pressure are in GPa.

r_s	T	Gasgun	S-G	CEICM-VMC	CEICM-DMC	GLE-VMC
2.202	2820	0.120	0.116	0.105(6)	0.10(5)	0.144(8)
2.1	4530	0.234	0.234	0.226(4)	0.225(3)	0.246(9)
1.8	3000	-	0.528	-	0.433(4)	0.410(8)

Proton-proton g(r) in molecular fluid

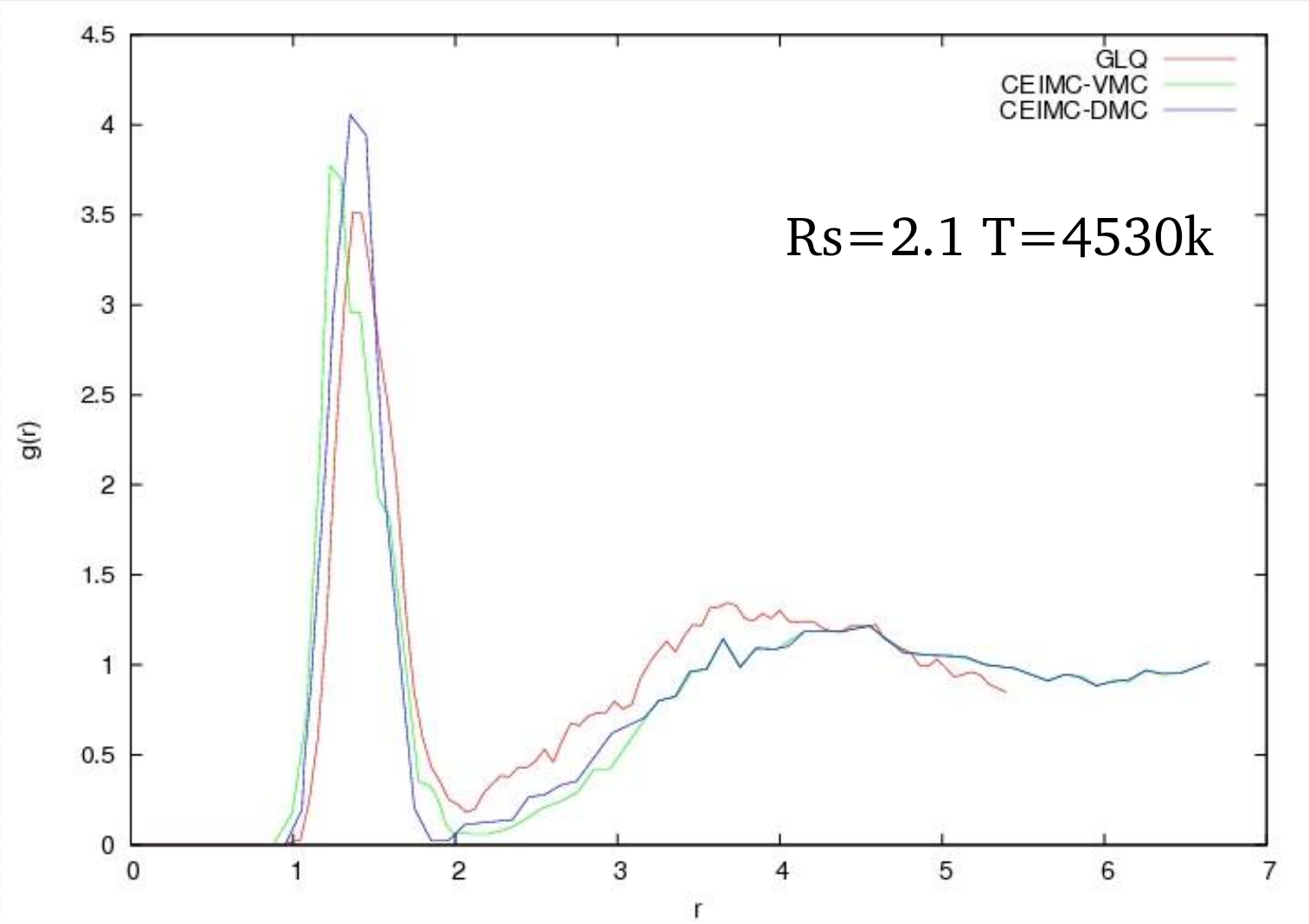

Proton-proton g(r) in molecular fluid

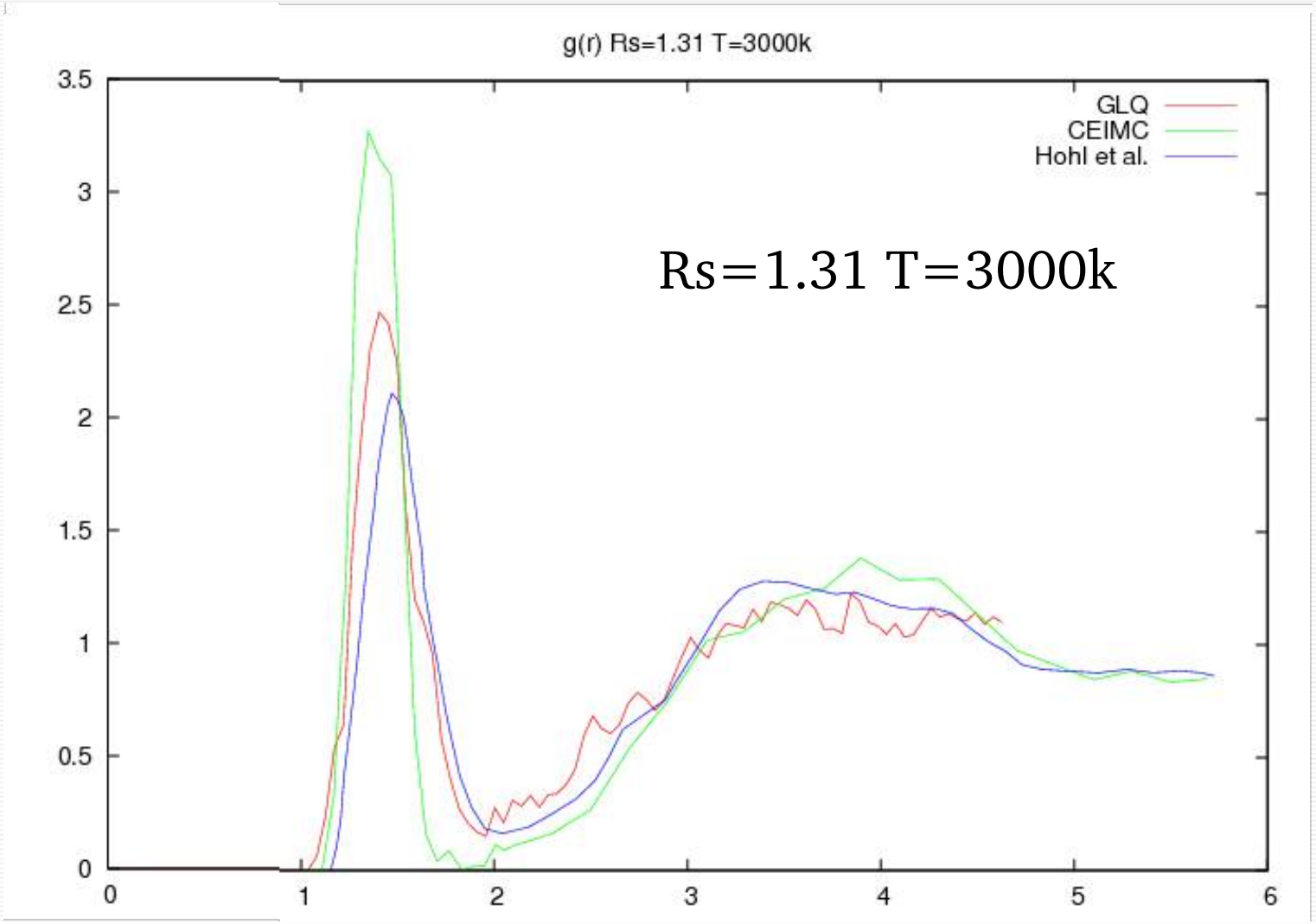

Condensation Energy

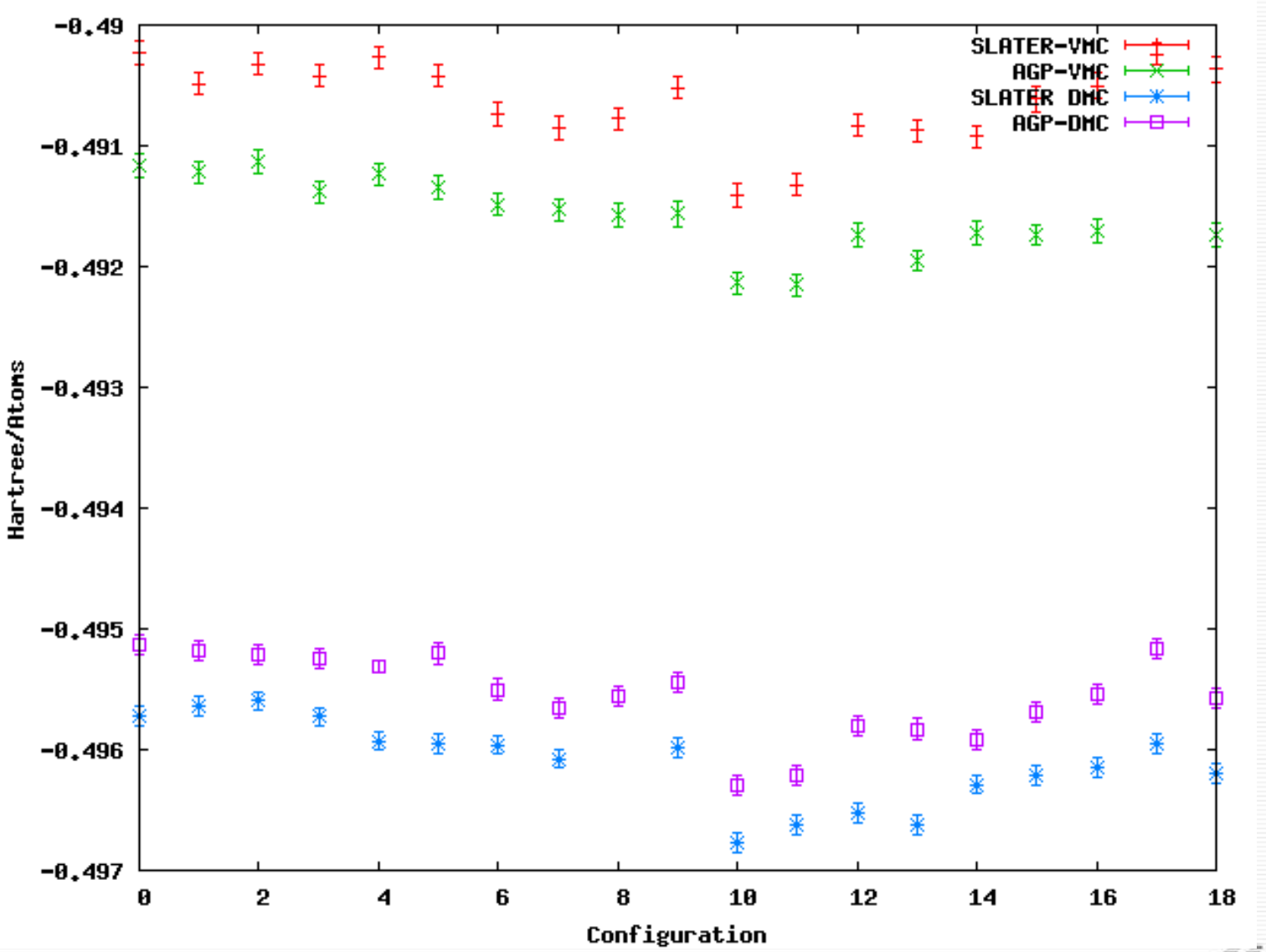

Off-Diagonal Long Range Order

two-body density matrix

$$\begin{aligned}\rho_2(x_1,x_2;x_1',x_2') &= \langle\Psi_N|a^+(x_1)a^+(x_2)a(x_1')a(x_2')|\Psi_N\rangle \\ Tr\rho_2 &= \frac{1}{2}\int \rho_2(x_1,x_2;x_1,x_2)dx_1dx_2 = \frac{N(N-1)}{2}\end{aligned}$$

ODLRO

$$\rho_2(x_1',x_2';x_1,x_2) = \alpha f^*(\vec{x}_1'-\vec{x}_2')f(\vec{x}_1-\vec{x}_2)$$
$$\text{for } |x_1-x_2|, |x_1'-x_2'| \le \xi \text{ and } |x_1-x_1'| \to \infty$$

projected two-body density matrix

$$h(x,\theta,\phi) = \frac{1}{N}\int dx_1dx_2\rho_2(x_1'+x,x_2'+x;x_1,x_2)$$

the estimator we used

$$h(x,\theta,\phi) = \frac{1}{M_c}\sum_{i<j\{r_{ij}<\xi\}} \frac{\Psi_t(r_1,r_2,...,r_i',...,r_j')}{\Psi(r_1,...,r_n)}$$

Eigenvalues of pair function

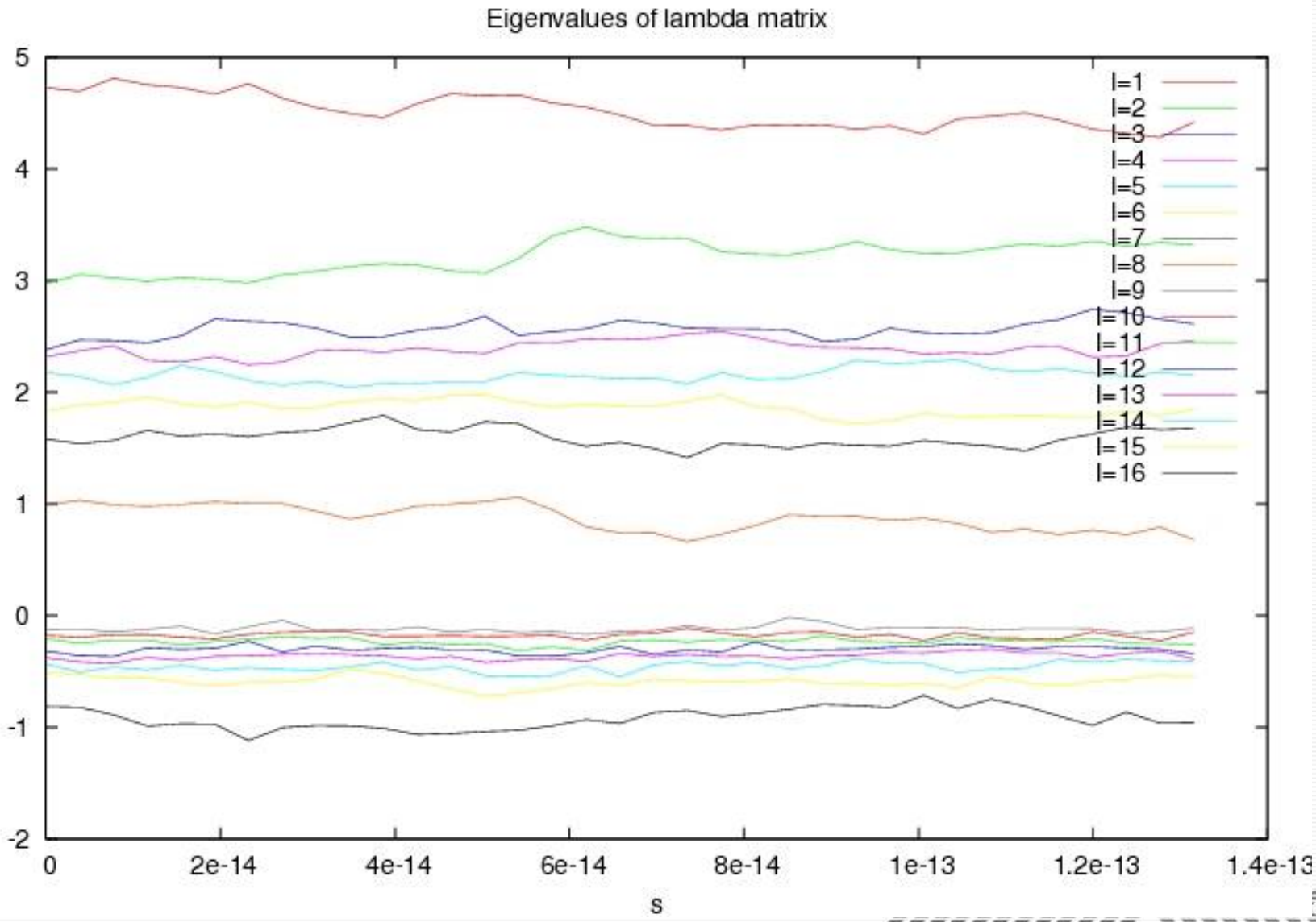

Superconductivity in high pressure hydrogen?

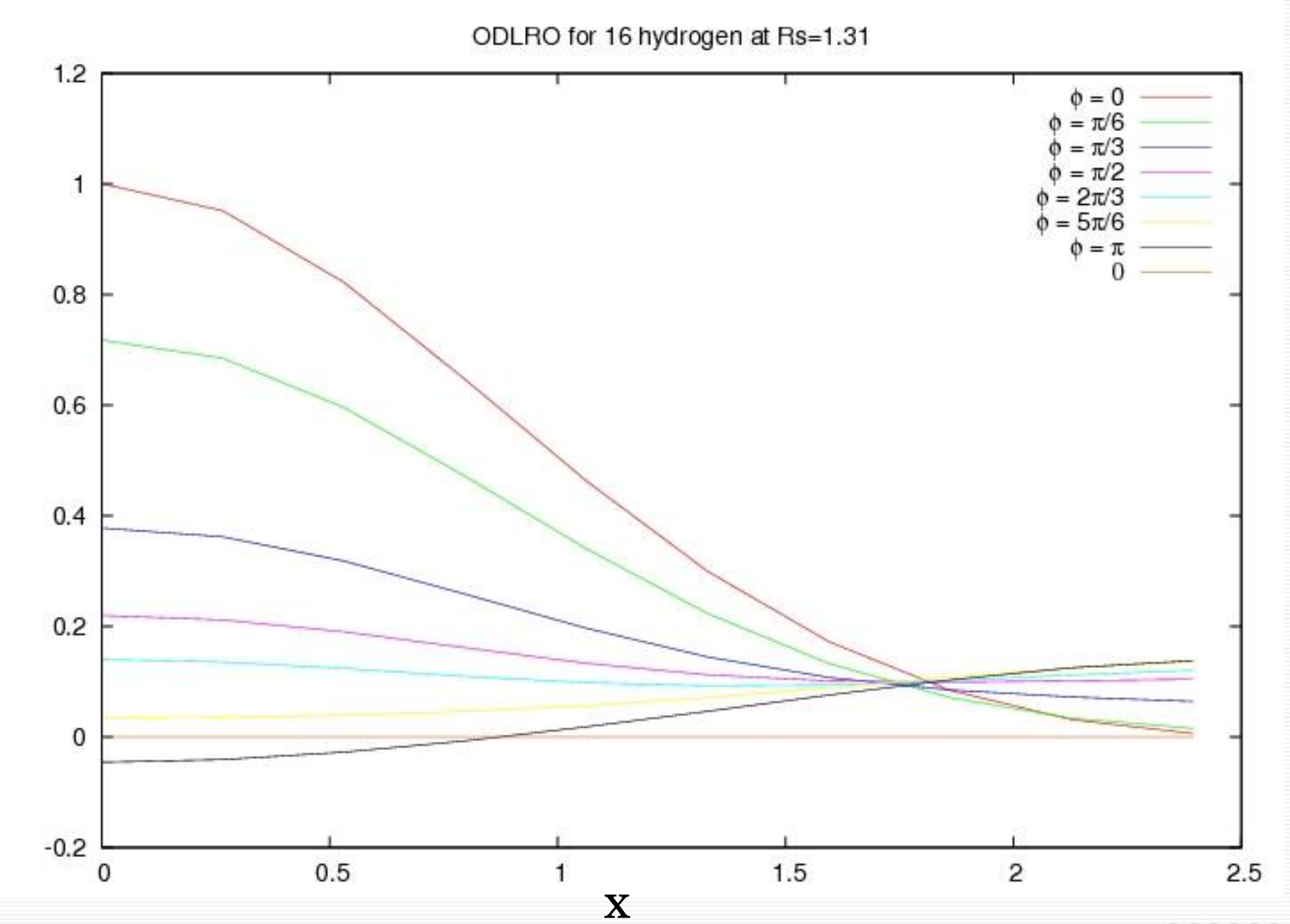

Condensation energy VS Size

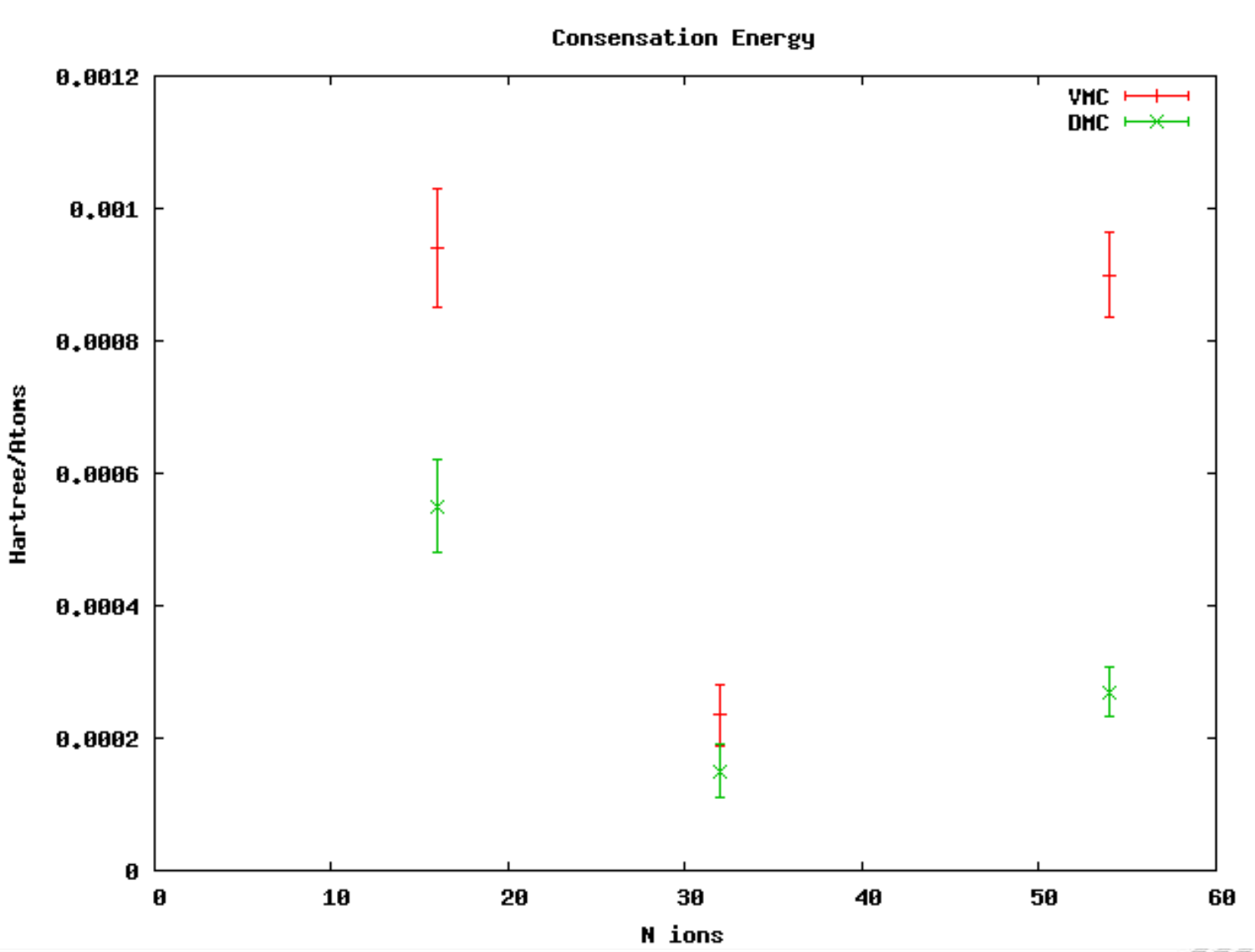

ODLRO for 54 hydrogen atoms at 300K

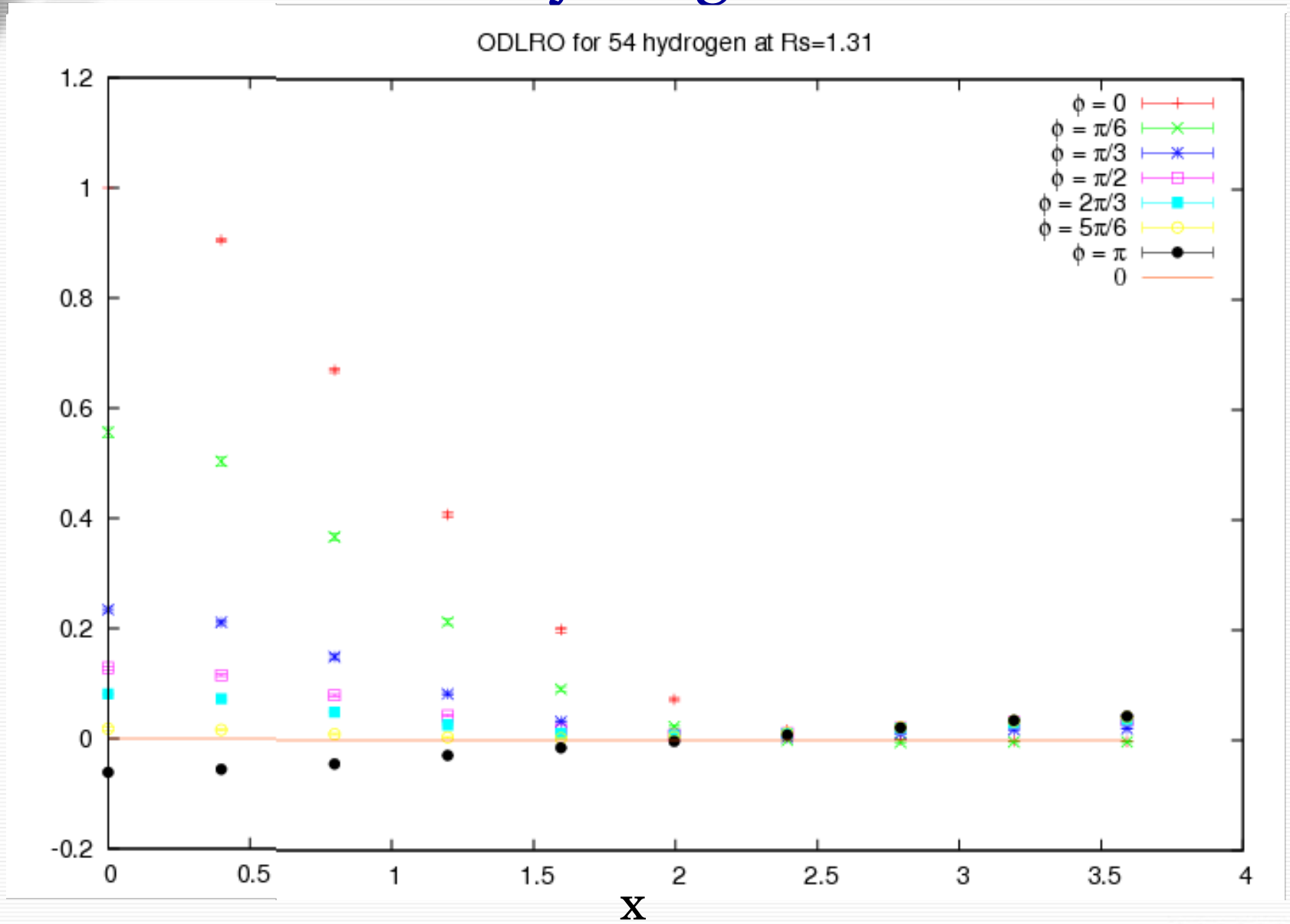

Conclusions

- A new highly correlated wave-function

JOURNAL OF CHEMICAL PHYSICS 121 (15): 7110-7126 OCT 15 2004
COMPUTER PHYSICS COMMUNICATIONS 169 (1-3): 386-393 JUL 1 2005

- A new technique to simulate finite temperature systems

ARTILE IN PREPARATION

- Full optimization during the ion dynamics

- RVB phase in High Pressure Hydrogen?

(ARTICLE?)

Future Work

(a lot things to do!)

GLQ technique:

- Reduction of the number of parameters
- Comparison with other methods (CEIMC ...)
- Improving the wave-function optimization
- Size effects and TABC
- Dynamic properties?

Other:

- Simulation of Molecular Hydrogen
- QM/MM with GLQ technique to simulate larger systems (biological)

Acknowledgement

Sandro Sorella

Michele Casula

Time-Step Error 2